Optical properties of RICH detectors

J. Va'vra

SLAC National Accelerator Laboratory, CA 94025, USA

Abstract – **In this review article[1] we discuss the optical components in RICH detectors. In particular we mention transmission and refraction index in gases, liquids, solids, optical glues, matching gels and Aerogel. We mention a few examples of mirror reflectivity in UV and visible region. We also discuss radiation damage, radio-luminescence, yellowing from light exposure, optical distortions in materials, and scintillation.**

INTRODUCTION

A beautiful thing about Cherenkov detectors is that their performance is basically determined by the refraction index, transparency of the medium, QE and angular resolution of photon detectors.

REFRACTION INDEX

One deals with two refraction indices. The "phase refraction index" is defined by: $n \equiv n_{phase} = c/v_{phase}$, where v_{phase} is waveform speed in the medium; it appeared first in the Snell's law. The "group refraction index" is defined by: $n_{group} = c/v_{group} = (n_{phase} - \lambda \cdot dn/d\lambda)$, where v_{group} is propagation velocity of wave energy.[2]
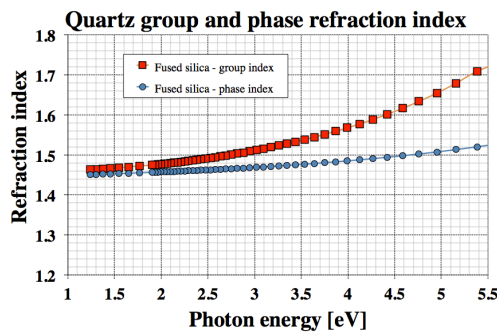
Fig. 1 Energy dependence of two refraction indices in the Fused silica.

Figure 1 shows a typical wavelength-dependent difference between two indices for the Fused silica; one can see that the energy propagates more slowly through a medium than the wave's phase, especially in far UV region. To determine the

phase refraction index, one starts from the Lorentz-Lorenz equation:

$$\frac{(n^2-1)}{(n^2+1)} = \alpha \cdot f(E) \qquad (1)$$

where $\alpha = 0.378(cm^3) \cdot [\rho (g \cdot cm^{-3})/M(g \cdot mole^{-1})]$ and f(E) is the molar refractivity, usually fitted with two-pole Sellmeier function:
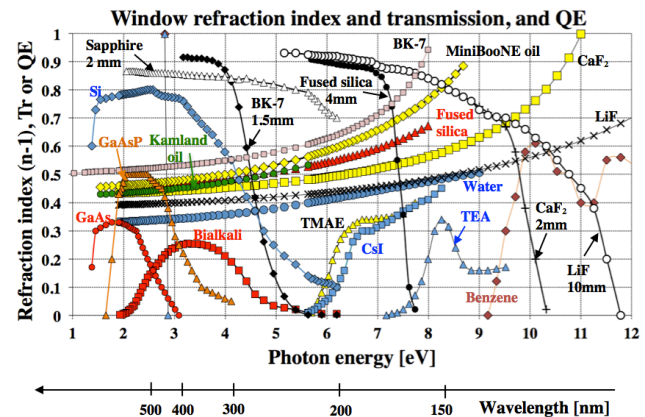
$$f(E) = \frac{F_A}{(E_A^2 - E^2)} + \frac{F_B}{(E_B^2 - E^2)} \qquad (2)$$

Numerical values of F_A, F_B, E_A and E_B for typical Cherenkov detector materials can be found in these two references [1,2].

One can now calculate many quantities. For example, a transmission (*Tr*) of thin a window of thickness (*L*) can be calculated using these two equations:

$$R = \frac{(n-1)^2}{(n+1)^2} , \ Tr = \frac{(1-R)^2 t}{1 + R^2 t^2} , \ t = e^{-\mu L} \qquad (3)$$

where (*R*) is reflectivity and (μ) is attenuation length.

Fig. 2 Refraction index (n-1), transmission (Tr) and quantum effeciency (QE) of typical windows, radiators and photocathodes. **Benzene** was used by HRS; **TMAE** by DELPHI, SLD, OMEGA, CERES, JETSET and CAPRICE; **TEA** by CLEO; **CsI** by ALICE, ATLAS, COMPASS, HADES; **Bialkali** by HERA-B, DIRC, HERMES, Belle-II, CELEX detectors.

Figure 2 shows a history over past 30 years of a refraction index (n-1) of various radiators, transmission (Tr) of typical window materials and the photocathode quantum effeciency (QE) as a function of wavelength and photon energy. Generally one can say that there was a steady trend in change of operating point over the past ~30 years: going from very far UV region, represented by the HRS experiment with the Benzene photocathode, all the way to visible wavelengths, as represented by the BaBar DIRC [3] using the Bialkali photocathode. There are two main reasons: (a) operational difficulties were reduced substantially using commercial Bialkali photocathodes, and (b) detectors had smaller chromatic errors.

An important group of radiator materials are Freon liquids $C_n F_{2n+2}$. Their refraction index can be described simply as

---

[1] Invited talk at RICH 2013, December 4, Kamakura, Japan
[2] Ibn Sahl, was the first astronomer to use the Snell's law accurately when building his lenses in Baghdad (940-1000 a.d.). The phase index was introduced by W. Snel van Royen (Willebrord Snellius), a Dutch astronomer (1580-1626). The group velocity concept was introduced ~200 years later by W. Hamilton, an Irish astronomer (1805–1865).

$n = a + b \cdot E$, for photon energy range $5 \leq E \leq 7$ eV, as shown on Fig. 3a [4]. During the ALICE experiment beam tests, a different slope was found for the C_6F_{14} liquid in the same energy interval: $n = 1.177 + 0.0172 \cdot \lambda$ (Å) [5].[3] This was followed by more measurements, and a summary is shown on Fig. 3b.[4] One can notice that the refraction index energy dependence is non-linear if a larger photon energy window is used.

(a)

(b)
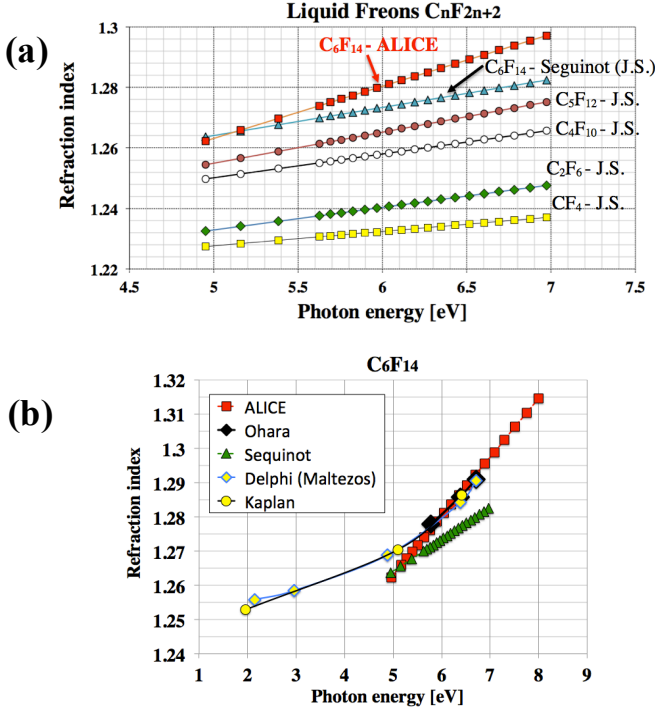
Fig. 3 (a) Refraction indices of various Freon liquids as measured by Delphi [3] and ALICE [4]. (b) Summary of all measurements for the C_6F_{14} liquid for a larger energy range. The refraction index does not follow a simple linear relationship if a larger photon energy window is used [4-7].

Table 1: Sellmeier parameters (2) for noble gases [2].

	H_2	He	Ne	N_2	Ar	Kr	Xe
E_A (eV)	12.88	22.389	17.419	13.414	13.084	11.50	8.885
E_B (eV)	20.25	40.412	45.501	26.216	24.217	17.789	25.358
F_A (eV^2)	638.899	451.532	278.088	921.282	791.68	851.667	813.157
F_B (eV^2)	653.230	788.718	3625.882	3659.598	3793.994	4034.683	10960.59

Table 1 shows constants for the Sellmeier function (2) for noble gases [2]. Refraction index of gas and liquid phase are related through equation (4), where p is gas pressure, T is temperature, R is a gas constant, M is molecular weight and ρ is a liquid density.

$$\frac{n^2-1}{n^2+2} = \left(\frac{p}{RT}\right)_{gas} \left(\frac{M}{\rho}\right)_{liq} \left(\frac{n^2-1}{n^2+2}\right)_{liq} \qquad (4)$$

A knowledge of the refraction index of various optical couplings between different materials is crucial for all optical designs as they influence the photon reflection, a phenomenon especially important at large incidence angles to glue/window interfaces. Figure 4a shows examples of refraction indices of

several coupling materials relative to the Fused silica. For example, BaBar DIRC bars were glued together with the Epotek-301-2 epoxy, the 1-st FDIRC prototype used the Kamland oil to couple to Fused Silica (one can see that it is pretty good match to Fused silica), final FDIRC prototype used Shin-Etsu RTV SES-403 to couple its optics to the DIRC bar boxes, Belle-II TOP counter is using Norland 61 epoxy, and Panda prototype used Marcol 82 mineral oil. Figures 3b&c show the measurement of the Epotek 301-2 optical epoxy and the Shin-Etsu SES-403 RTV. As one can see, some people use uncured epoxy, cured epoxy is made in a form of a wedge to enable laser-based deflection measurements.


(a)

(b)

(c)
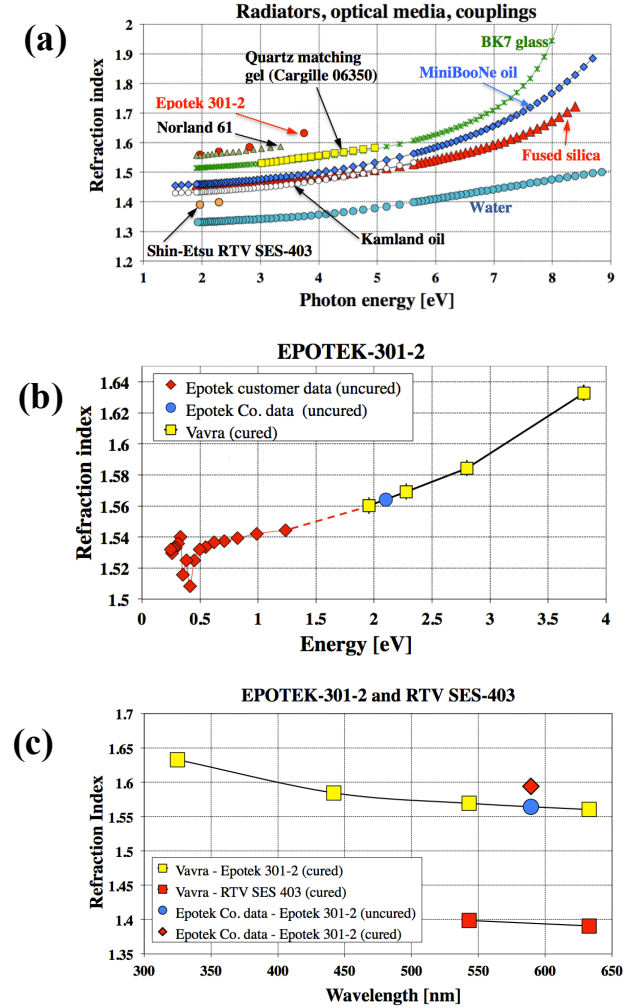
Fig. 4 (a) Refraction index of Epotek-301-2 optical epoxy over a large energy range, some data taken in a liquid form, and some cured into a prism shape to allow a laser-based measurement. (b) Epotek-301-2 optical epoxy and Shin-Etsu SES-403 RTV in the DIRC wavelength range. (c) Refraction indices of some coupling materials relative to the Fused silica [8].

Fig. 5 shows the refraction index of the K_2CsSb Bialkali photocathode, which can also influence reflection and absorption [9]. Its real part (**n**) describes the phase refraction index, and the imaginary part (**k**) describes the absorption.

---

[3] Both STAR and ALICE experiments are using this new parameterization.
[4] ALICE group asked Ohara Co. to measure the C_6F_{14} refraction index. Their values were found to be consistent with data of Maltezos [6], Kaplan [7].
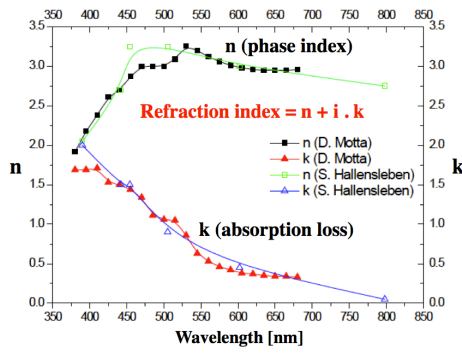
Fig. 5 Refraction index of a K_2CsSb Bialkali photocathode. The real part **n** is the phase refraction index, the imaginary part **k** describes the absorption [9].
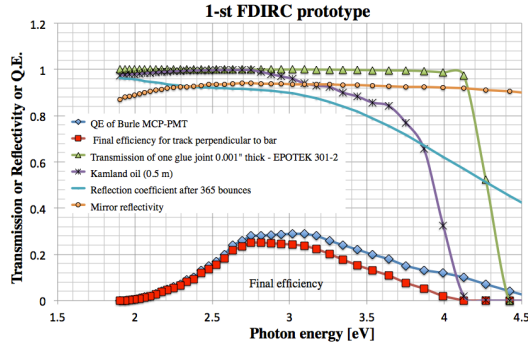

Fig. 6 The energy acceptance of 1-st FDIRC prototype [10]. The limit to the acceptance from the low energy side is the photocathode QE, and from the higher energy side (a) reflectivity of quartz for 365 bounces, and (b) Kamland oil transmission for 50 cm. The error $\sigma_E \sim 1eV/2.35 \sim 0.42$ eV.

The refraction index is influencing the chromatic broadening of the Cherenkov angle, which is typically limiting the performance. The chromatic error contribution to the Cherenkov angle σ_{θ_c} is calculated by differentiating equations "$\cos \theta_c = 1/\beta \, n(E)$", and the Lorents-Lorenz equation (1) [1]:

$$\sigma_{\theta_c} = \frac{\partial \theta}{\partial n}\frac{dn}{dE}\sigma_E = \left(\frac{1}{n \tan\theta}\right)\left(\alpha\frac{(n^2+2)^2}{6\,n}\frac{df}{dE}\right)\sigma_E \qquad (5)$$

The chromatic error is reduced by reducing dn/dE and σ_E. A decreasing σ_E results in a decreased number of photoelectrons. The best way to reduce the chromatic error is by choosing a detector with a longer wavelength response. The error σ_E is determined by the detector overall response. For example, Fig. 6 shows energy response of FWHM~1eV for the 1-st FDIRC prototype [10], and equation (5) gives σ_{θ_c} ~ 4.5 mrads.

New fast DIRC-like RICH detectors can correct the chromatic error using timing – see Fig.7. This idea was pioneered for the first time by the 1-st FDIRC prototype [10]. Figure 7a,b shows the principle. A red photon is faster than the blue photon and their time of arrival to a given pixel can be measured with a fast detector. One can determine a correlation between $d\theta_c = \theta_c(\lambda) - \theta_c(\lambda_{ref})$ and $dTOP/L_{path} = TOP/L_{path}(\lambda) - TOP/L_{path}(\lambda_{ref})$, where TOP is time of propagation in quartz, L_{path} is photon path length and λ_{ref} is a refence wavelength, taken in the middle of acceptance. If the Cherenkov angle is measured well ($\sigma(\theta_c) \sim 10$mrad) with timing resolution of ~200ps or better, one can correct the chromatic error. One can reduce the Cherenkov angle error by ~1mrad typically.
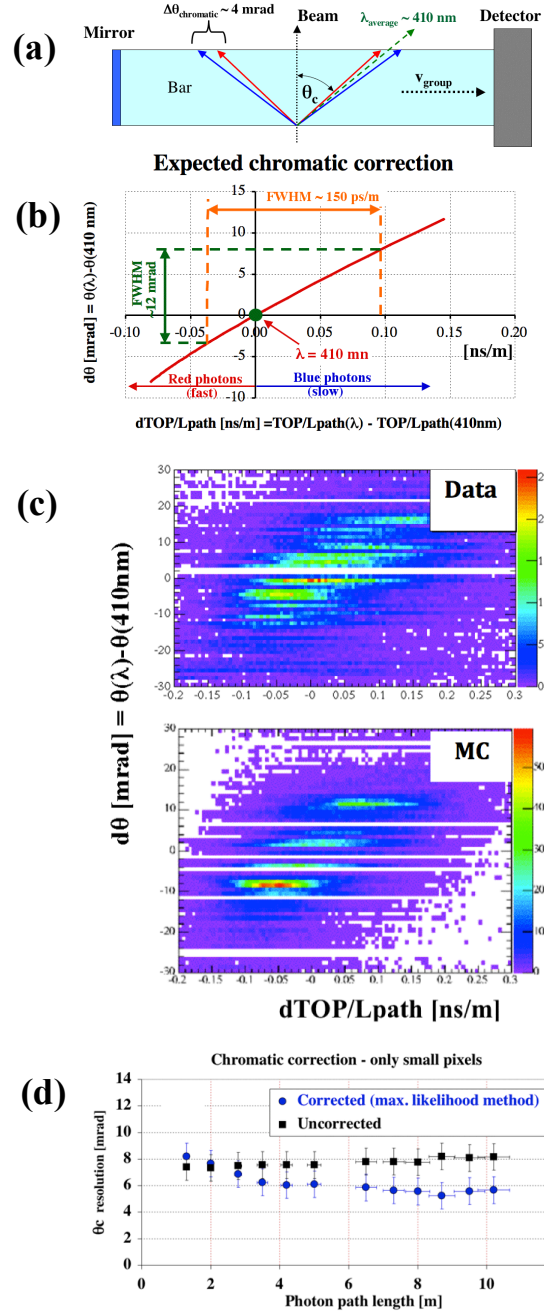

Fig. 7 (a) Red Cherenkov photons arrive earlier than blue photons in spite of an intial slight advantage. (b) A correlation between $d\theta_c = \theta_c(\lambda) - \theta_c(\lambda_{ref})$ and $dTOP/L_{path} = TOP/L_{path}(\lambda) - TOP/L_{path}(\lambda_{ref})$. (c) The same correlation shown for the data and the Geant 4 MC simulation. (d) Corrected and uncorrected Cherenkov angle resolution for 3mm pixels as a function of photon path length. One obtains about ~1mrad improvement on average by doing the chromatic correction by timing [10].[5]

TRANSPARENCY OF A MEDIUM

To achieve a good UV medium transparency is often a highly non-trivial problem. In case of gases and liquids, it requires mastering sophisticated filtering methods, which requires many years of experience, and understanding possible

---

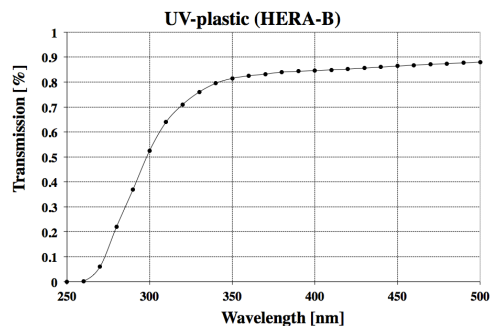[5] Similar results obtained with the final FDIRC prototype (talk by D. Roberts).

impurities. Figures 8a,b,c illustrate this problem in case of liquid Freons such as C_4F_{10}, C_5F_{12} and C_6F_{14}. The first experiments to use them on a larger scale was Delphi and CRID at SLD. But it took 10-15 years to achieve the ultimate purity in experiments such as STAR,[6] ALICE and COMPASS. One can summarize the improvements[7] as follows: (a) one can buy now much cleaner C_6F_{14} (PF5060-DL quality), (b) change molecular sieve size from 13X down to 4 or 5 Å, (c) use "copper catalysts", (d) avoid using Oxisorbs as it could react with partially fluorinated contaminants, (e) use N_2 gas to bubble through C_6F_{14} to remove oxygen, and (f) use stainless steel tubing. Delphi already avoided Oxisorbs [16], as they did not get consistent results, but CRID did use Oxisorbs to clean the C_6F_{14} liquid, which may have been a mistake - see Fig. 8b. Figure 8c shows a level of depth one has to go into to understand the C_4F_{10} transparency quantitatively.

(a)

(b)

(c)
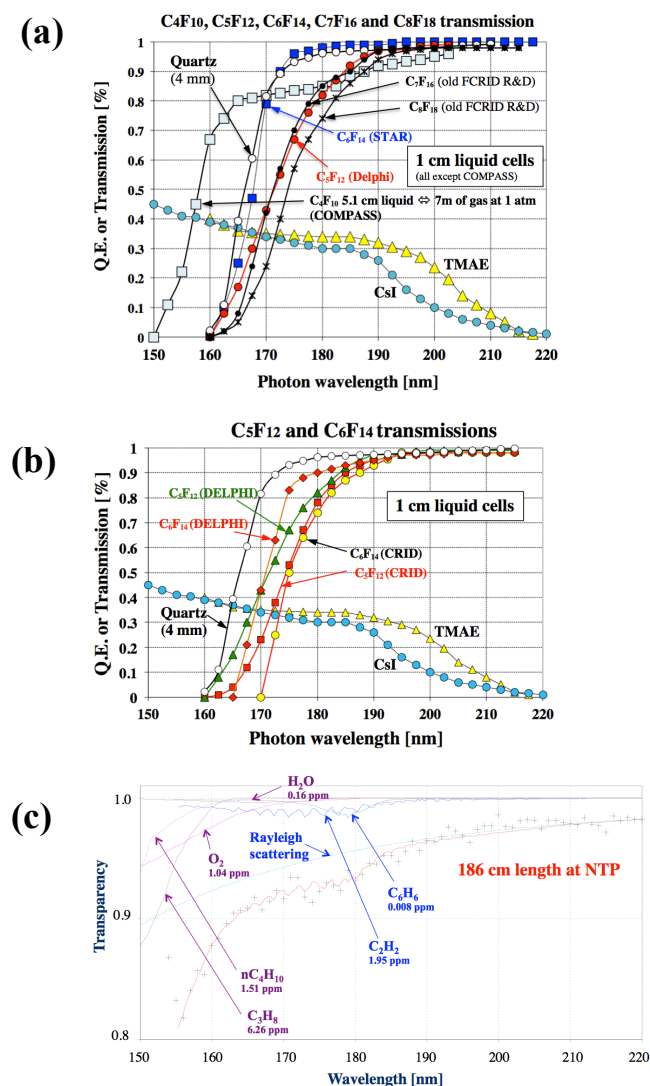
Fig. 8 (a) Transmission of various C_nF_{2n+2} Freon liquid radiators. We quote only the best achieved results [10-12], [5]. (b) The transmission of C_5F_{12} & C_6F_{14} achieved only ~15 years earlier [14-15]. (c) Reconstruction of measured C_4F_{10} transmission by fitting contributions from various contaminants [16].

Fig. 9 Transmission of 3-mm thick UV-plastic, used for HERA-B photon camera lenses [17].

One can consider a UV-plastic for certain applications. For example, the HERA-B experiment used such plastic for the photon camera lenses [17] with a good transmission – see Fig. 9. Light collection system had these features: (a) by using aspheric lenses off-axis distortions were minimized, (b) easy to fabricate, (c) molded production is cheap, (d) were able to handle high HERA-B rates, after TMAE-based detector failed due to aging.
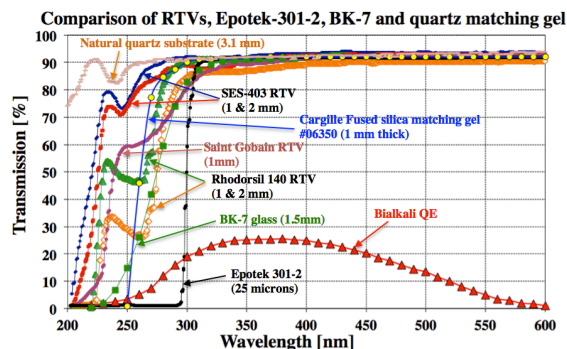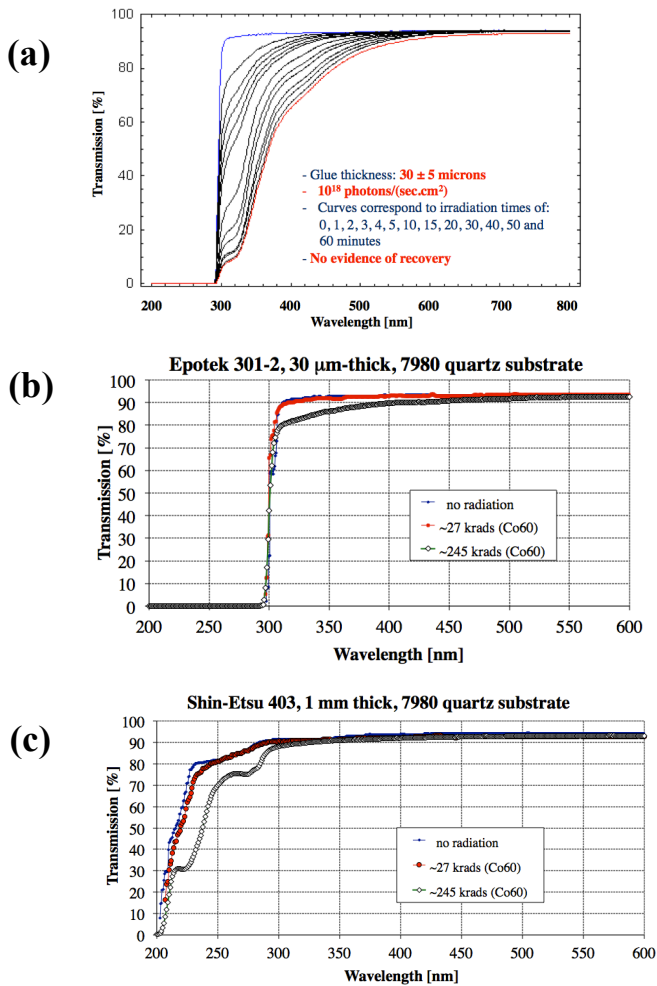
Fig. 10 Transmission of several RTVs, Epotek-301-2 optical epoxy, Fused silica matching gel, all relative to the the transmission of a quartz substrate [18]. We also show BK-7 glass and the Bialkali photocathode QE. Each glue samle was imbedded between two 3.1 mm-thick quartz pieces made of natural quartz.

Figure 10 shows a transparency of several optical glues considered for FDIRC for SuperB [18]. One can see that a 1mm-thick RTV samples Rhodorsil 141 or Shin-Etsu SES-403, are very transparent. The Epotek 301-2 epoxy limits the DIRC optical acceptance.

As Fig. 11a shows, the Epotek-301-2 optical epoxy can be damaged by UV photons,[8] if one exceed a limit of ~10^{19} photons/cm^2 [19]; the damage by Co^{60} is shown on Fig. 11b [18]. Detailed anlysis of the BaBar DIRC data found no evidence that the Epotek glue was affected by radiation during a period of ~10 years.[9] One should nevertheless worry about damaging the instrument like this during machine physics runs. Fig. 11c shows that Shin-Etsu 403 RTV can be damaged also [18].

---

[6] The STAR collaboration benefited from a collaboration from several Delphi people, who had a long-term experience with the Freon purification.
[7] I thank for these comments to A. Di Mauro and M. Davenport.

[8] During the DIRC R&D effort, we have noticed that the Epotek-301-2 optical epoxy will yellow just sitting in the lab under fluorescent light.
[9] BaBar DIRC data analysis performed by N. Arnaud.

(a)

- Glue thickness: **30 ± 5 microns**
- 10^{18} photons/(sec.cm^2)
- Curves correspond to irradiation times of: 0, 1, 2, 3, 4, 5, 10, 15, 20, 30, 40, 50 and 60 minutes
- **No evidence of recovery**

(b) Epotek 301-2, 30 μm-thick, 7980 quartz substrate

- no radiation
- ~27 krads (Co60)
- ~245 krads (Co60)

(c) Shin-Etsu 403, 1 mm thick, 7980 quartz substrate

- no radiation
- ~27 krads (Co60)
- ~245 krads (Co60)

Fig. 11 (a) Epotek-301-2 optical epoxy transmission damage by photons [19]. (b) Epotek-301-2 damage by Co^{60} [20]. (c) Shin-Etsu 403 RTV damage by Co^{60} [18]. Samples in (b) and (c) used Corning 7980 fused silica substrate [18].

Fused silica is far from a "unique material", as there are many different grades available, with various different additives and impurities, different transmittances in different ranges of the wavelength spectrum. Figure 12 shows an example of this complexity. For example, the "wet" fused silica, with a large amount of OH-molecules, is suitble for working in the UV regime such as DIRC, on the other hand, the "dry" fused silica, with no OH-content and mimimum of other impurities, is useful for IR regime for fiber applications. For "wet" fused silica absorption in the IR regime is domination by OH-absorption peaks. Both DIRC Spectrosil-2000 bars or FDIRC's Corning 7980 are made of so called "wet' quartz; Corning 7980 is loaded with 800-1000ppm of OH-molecules, while other impurities are less than 1ppm. For this type of Fused silica the transmission is dominated by the Rayleigh scattering below ~600nm.

As one can see in Table 2, the radiation damage of Fused silica is also complicated. Generally more pure materials have lower damage. Typically natural quartz, such as used in the CRID experiment [14], has a severe radiation damage and such material is not suitable for modern high luminosity machines. However, even ultra-pure silica SiO_2 is sensitive to breakage of O-links by UV light and radiation. Once the O-

bond is broken, such molecule tend to create the color center, unless the glass has plenty of hydrogen around, which tends to fill the missing void. If hydrogen fills the void to form the SiOH molecule, the quartz remains transparent. It is a kind of "repair", which becomes effective if the quartz is loaded by at least ~10^{17} H-atoms/cm^3. For example, Corning 7980 Fused Silica, used for the FDIRC camera optics intended for SuperB, has 800-1000ppm of OH-molecular content (by weight), and less than 1000ppb of other impurities. M. Hoek's transmission measurements are consistent with the above point, but he makes an additional point that adding too much of hydrogen may affect the transmission negatively [20].
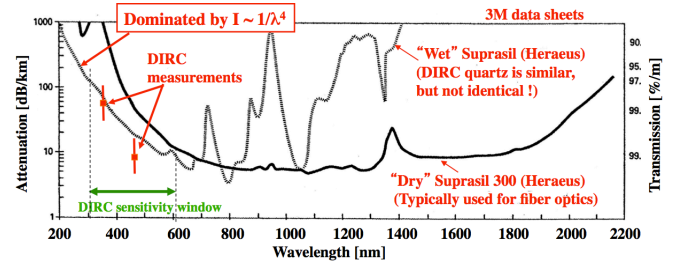
Fig. 12 Attenuation in dB/km or transmission in %/m of Fused silica. (a) Solid line: "Dry" Suprasil 300 or similar type of quartz is typically used in fiber optics and is optimized for the best transmission at around 1400-1600nm. (b) Dotted line: "Wet" Suprasil is optimized for the best transmission in the UV region; in addition, it is loaded by hydroxil (OH) to reduce the UV sensitivity and to improve the radiation hardness.

Table 2: Radiation damage by Co^{60} of various Fused silica materials [21].

Material	Manufacturer	Type	Visual change	Radioluminescence	Transmission loss
Vitreosil-F	TSL	Natural	No (100 krad)	No (100 krad)	Severe (7 krad)
T-08	Heraeus Amersil	Natural	Yellow (330 krad)	Yes (330 krad)	Severe (10 krad)
JGS3-IR	Beijing Institute	Natural	Brown (400 krad)	No (400 krad)	Severe (20 krad)
Suprasil	Heraeus Amersil	Synthetic	No (280 krad)	Yes (280 krad)	Small (280 krad)
JGS1-UV	Beijing Institute	Synthetic	No (650 krad)	No (650 krad)	No (650 krad)
Spectrosil 2000	TSL	Synthetic	No (180 krad)	No (180 krad)	Small (180 krad)
Spectrosil B	TSL	Synthetic	No (254 krad)	Yes (254 krad)	Small (254 krad)

(a)

(b) Int. reflection coeff. =f(wavelength)

- SLAC (1999)
- Panda (2013)
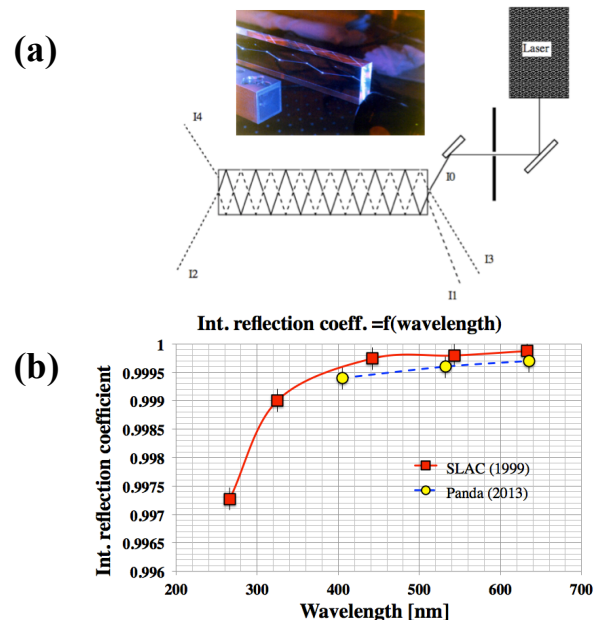
Fig. 13 (a) Experimental setup to measure the internal reflection coefficient by measuring 5 intensities [21]. (b) Internal reflection coefficient obtained in the DIRC setup [22], compared with Panda measurement with somewhat worse bar surface polish [23].

INTERNAL REFLECTION COEFFICIENT

DIRC-like detectors have to deal with a large number of internal reflections (up to 1500), and to have acceptable losses, one requires a very high internal reflection coefficient close to ~0.9997. This can be achieved if a Fused silica bar is polished to ~5Å rms. The internal reflection coefficient was measured absolutely with a ''calorimetric'' method [21]. As shown in Fig. 13, this method measures five light intensities and uses the number of light bounces, the bar dimensions and the bulk attenuation as inputs.

The internal reflection coefficient has a direct effect on the wavelength acceptance in the DIRC-like devices. For photons with many bounces, the wavelength response shifts toward red wavelengths. Figure 14 shows this effect, calculated for 100, 500 and 1000 bounces for the 1-st FDIRC prototype [10].
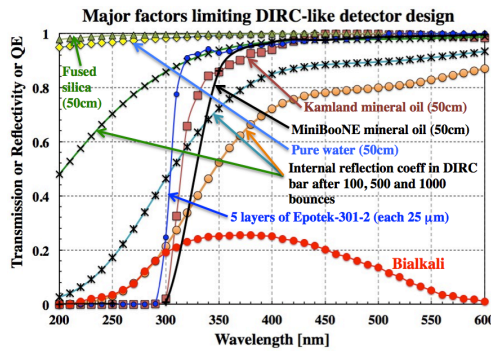
Fig. 14 The internal reflection coefficient starts limiting the transmission of DIRC-like detectors, such as the FDIRC prototype, for a large number of photon bounces – the detector becomes more and more sensitive to red wavelengths [10].
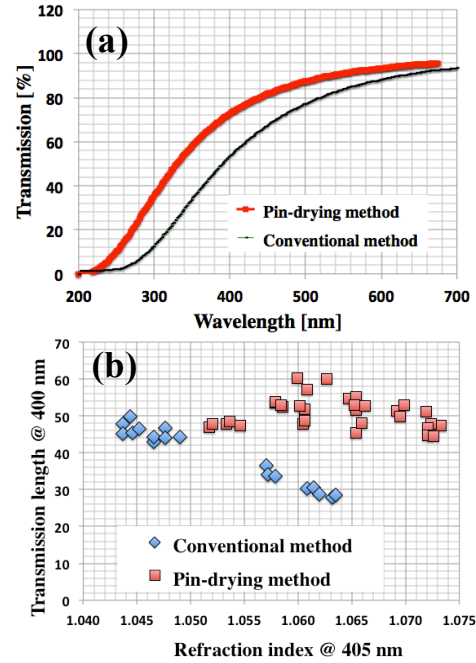
AEROGEL

The Aerogel[10] has a long history of development, a process, which is still continuing to this date more than 80 years after the invention. It is the best insulator and lowest density solid material. Since the refraction index follows the eqation is n = k ρ, one can reach very small values n = 1.008-1.15 (k = 0.213 at 400nm). There two important quantities to consider: (a) scattering length L_{scatt}, which is determined by internal structure (pores) and follows the Rayleigh law, and (b) absorption length L_{abs}, which is controlled by impurities; generally $L_{abs} >> L_{scatt}$.

The chemical structure is SiO_2 with small 1-5% contamination of the water depending on the baking procedure. The atomic and nuclear properties of aerogels are almost the same as for quartz. By modifying the Aerogel chemistry, one can control a number and size of pores, and in this way one can control the Aerogel transparency.

Figure 15 shows an example of a technique, so called pin-drying technique, which seems to improve the Rayleigh[11] UV-

---

[10] Aerogel was invented in 1931 by Samuel S.Kistler, American scientist and chemical engineer, (1900-1975)

[11] Lord Rayleigh (John William Strutt), (1842–1919)

edge transparency and the transmission length of the Aerogel [22].

Fig. 15 (a) Transmittance and (b) transmission length at 400 nm for conventional method and so called pin drying technique to prepare Aerogel, as obtained in the Belle-II R&D effort [24].
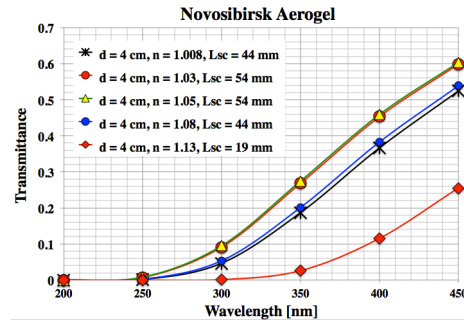
Fig. 16 (a) Transmittance of 4cm-thick Aerogel tile for various types materials of different refraction index and the scattering length, as obtained in the Novosibirsk R&D effort [25]. The transmittance is clearly considerably worse than what would obtain from the Fused silica.

For Aerogel, the Rayleigh scattering occurs on particles of diameter "d" consiting of solid ball clumps of SiO_2 separated by voids (pores), and follows the formula (valid for $\pi d << \lambda$, which is easily satisfied since d < 10 nm typically):

$$I = \frac{1+\cos^2\theta}{2R^2}\left(\frac{2\pi}{\lambda}\right)^4\left(\frac{n^2-1}{n^2+2}\right)^2\left(\frac{d}{2}\right)^6 \qquad (6)$$

To minimize the scattering, one minimizes the diameter d. One should point out that the Aerogel formula for the Rayleigh scattering for solid Fused silica differs from equation (6), as it is due to scattering on molecules (SiO_2), and follows this equation:

$$I = I_0\frac{8\pi\alpha^2}{\lambda^4 R^2}(1+cos^2\theta) \qquad (7)$$

One seeks a good ratio of "unscattered Cherenkov photons" to "scattered photons."

The transmittance (Tr) and the scattering length (L_{scatt}) are related to ech other as folows:

$$Tr = A \exp\left[x/L_{scatt} \, (\lambda/400)^4\right]$$

where x is the Aerogel thickness, A is the surface scattering coefficient (0.9-0.96) [25]. To achieve a good N_{pe}/ring ratio, the aerogel tile thickness should to be at least 4 cm, and for this thickness the scattering length is a significant factor in the transmittance. This is illustrated in Fig.16, which shows that the transmittance of 4 cm-thick Aerogel tiles are considerably worse than what one would get from Fused silica of the same thickness.

A significant new improvement,[12] utilizing the Aerogel detector concept, first published in Ref. [27], is stacking together several layers of Aerogel tiles (see Fig.17), each with different refraction index, to achieve a focusing effect, and therefore improve the Cherenkov ring resolution. Several groups have now accepted this concept [24, 26, 27].

Fig. 17 A stack of five Aerogel tiles, each one with different refraction index, to achieve focusing [26].

MIRRORS

Figure 18 shows four examples of mirror reflectivity from four different applications. It is clear that mirrors operating in visible range are relatively straightforward, however, mirrors operating in far-UV are the most difficult to use – see Fig. 18c.

<hr/>

[12] The idea was originally introduced independently by T. Iijima and by S. Korpar.
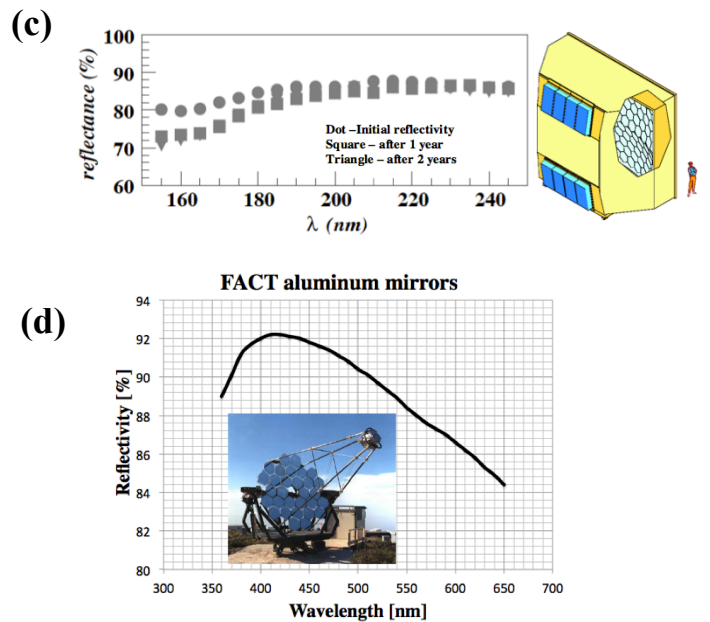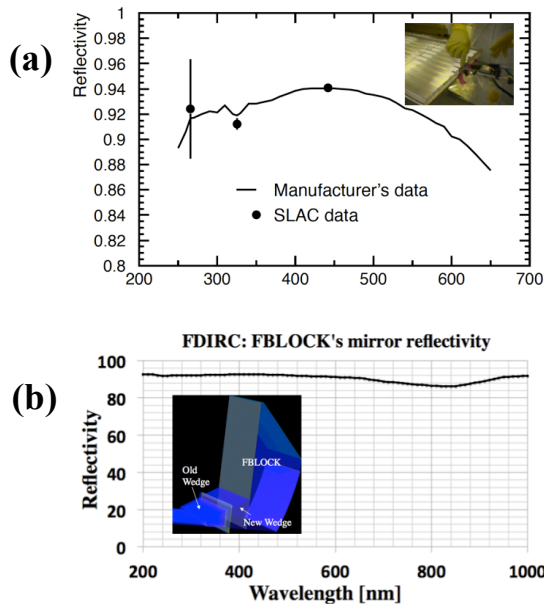
Fig. 18 Mirror reflectivity for (a) BaBar DIRC at the end of each bar (external reflectivity mirror) [21], (b) FDIRC focusing block internal reflectivity mirrors [28], (c) COMPASS mirrros operating in far-UV regime [29], and (d) FACT aluminum mirrors working in air [30].

OPTICAL ABBERATIONS

We would like to conclude the paper by mentioning two optical effects one should be aware of when designing fused silica optics.

The first effect is a diffraction-like pattern, called ''lobes', observed in early DIRC bars [21]. Fig. 19a shows a model of the structure of the optical inhomogeneity, where it is assumed that there are curved ''layers'' of varying index of refraction within the fused silica ingots from which the bars are produced – see Fig.19b. If a laser beam were traveling tangent to these layers, then it would, in effect, see a ''diffraction grating'' formed by the alternating layers of high and low refraction index, thereby producing lobes – see Fig.19c. This effect is observed in many early samples of both types of synthetic fused silica considered for use in the DIRC: Heraeus Suprasil and QPC Spectrosil. The ''lobe effect'' must be taken very seriously because it can cause photon losses or image distortion of the Cherenkov light. Because of its bright lobes and the angular range over which they are produced, Heraeus Suprasil was rejected for use in the DIRC. QPC Spectrosil fused silica was deemed acceptable both because of its lower lobe power and also since the lobes in the QPC fused silica are only produced at angles close to perpendicular to the bar axis, which are not relevant for the photons detected in the DIRC.

The fused silica material's optical inhomogeniety has improved considerably since the DIRC construction, thanks to improvements in the lithography. For example, the FDIRC camera optics [31] used the Corning 7980 fused silica, which had the refraction index variation of less than 10 ppm – see Fig.20. No lobes were observed with a laser.

The second effect we want to mention is so called kaleidoscopic effect discovered during the 1-st FDIRC

prototype R&D effort [10]. The optical aberration ranges from 0 mrad (at ring center) to ~9 mrad (in outer wings of Cherenkov ring), i.e., it is a significant effect, comparable to the chromatic error in magnitude, and has to be considered seriously. Figure 21a show the anatomy of the Cherenkov ring images for z-positions along the bar length. We tried to reduce the kaleidoscopic effect with various types of focusing with no success [33] – see Fig.21b. Even non-focusing DIRC has it, uniformly spread along the ring. It will be interesting if one come up with an optical design, which will remove this abberation.
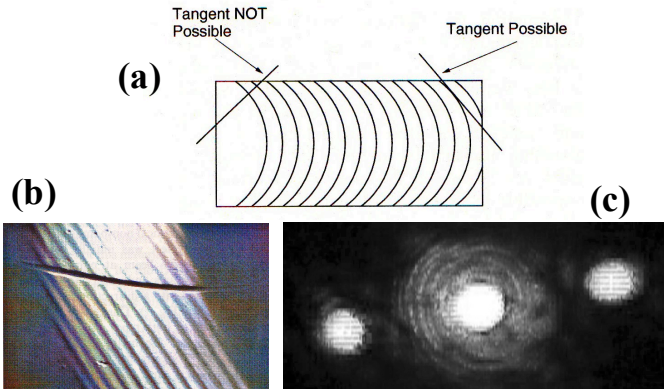
Fig. 19 (a) Model of the periodic structure of the optical inhomogeneity within raw ingot, (b) actual periodicity observed under the microscope (with overlayed 7μm wire), and (c) observed diffracion with a laser [21].
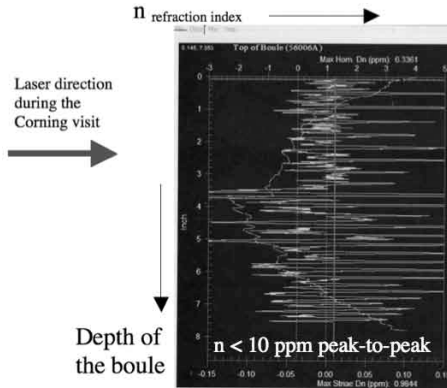
Fig. 20 FDIRC camera [31] optics used Corning 7980 fused silica, which had the refraction index variation of less than 10 ppm.[13] Although refraction index has a modulation, no lasrer difraction was observed in this material [32].

SCINTILLATION AND RADIO-LUMINESCENCE

It is not desirable if a radiator scintillates when charged particles are passing through. Ref.[34] did show that CF_4 gas radiator scintillates the most of typical gases – see Fig. 22. This is due to emissions from molecular fragments $F*$ and CF_3* [35].

A considerable effort was spent during the DIRC R&D

stage to prove that the DIRC bar fused silica does not scintillate when a muon traverses the bar [36].

In addition to transmission loss, radio-luminescence was also observed in quartz as consequences of radiation damage; Table 2 summarizes all these observations [21]. The radio-luminescence is a known property of quartz and fused silica [37]. This effect was found to be negligible for the DIRC final fused silica choice [21].
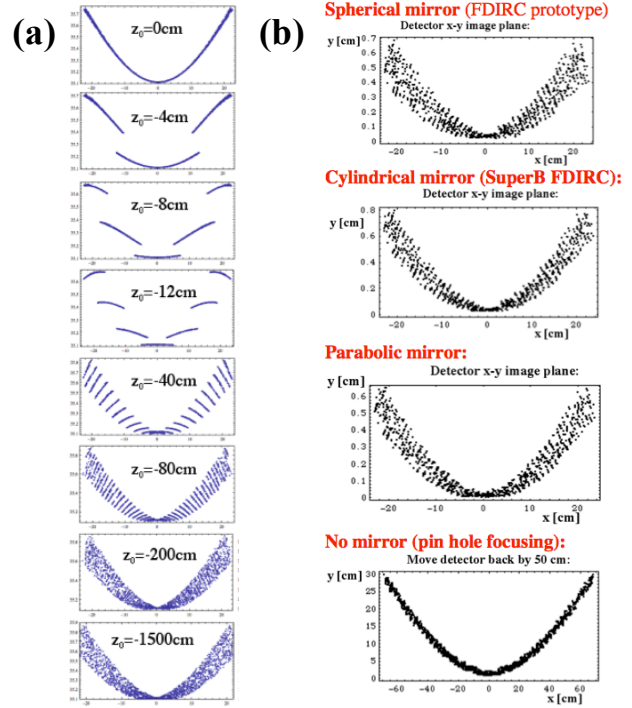
Fig. 21 (a) Cherenkov ring images at a dip angle of 90° as a function of track distance along the bar length, starting at z = 0, closest point to the focusing block. Number of kaleidoscopic images grows step by step [31]. (b) Kaleidoscopic images for different mirrors in FDIRC camera and BaBar DIRC (no mirror) [10].

Fig. 22 Scintillation in various gases. Notice that CF_4 gas scintillates the most [34]. Photon excitations were stimulated by proton (E_p = 22 MeV), O^{16} (E_O = 80 MeV) ion beams, and α's from Am^{241} source (E_α = 5.485 MeV).
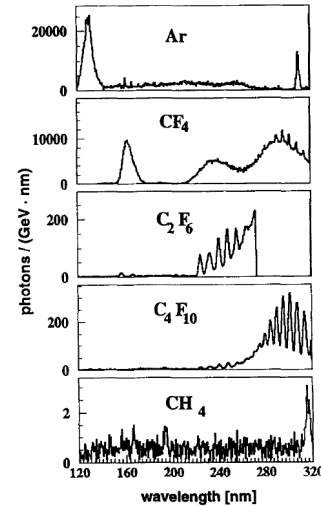
---

[13] The most expensive Corning fused silica material, used in the lithography, has the refraction index variation of less than 0.1 ppm. This level was judged as unnecessary for the FDIRC camera.

REFERENCES

[1] T.Ypsilantis and J. Seguinot, Nucl.Instr.& Meth. A 343 (1994) 30.

[2] E. Nappi and J. Seguinot, Riv. del Nuovo Cimento, Vol. 28, N. 8-9, 2005.

[3] B. Ratcliff, SLAC-PUB-5946 (1992), SLAC-PUB-6047 (1993).

[4] J.Seguinot et al., CERN-LEPC 82-59, DELPHI 82-23, CERN-EP/89-92
    and LPC/89-25.

[5] A. Di Mauro (ALICE), Nucl. Instr. and Meth. A 433 (1999) 190.

[6] Maltezos, J. of Modern Optics, 2000, Vol. 47, no. 10, 1693.

[7] Y. Andres et al., Nucl.Instr.& Meth. A 486 (2002) 590.

[8] J. Va'vra, DIRC note 132, July 2001.

[9] S. Hallensleben et al., Optical Communication,180 (2000) 89,
    D. Motta and S. Schonert, Nucl. Instr. and Meth. A 539 (2005) 217.

[10] 1st FDIRC prototype: J.F. Benitez et al., Nucl. Instr. and Meth. A
    595(2008)104, and K. Nishimura et al., Nucl. Instr. and Meth. A
    A701(2013)115-126.

[11] Y. Andres et al. (STAR), Nucl. Instr. and Meth. A 486 (2002) 590.

[12] Albrecht at al. (COMPASS), Nucl. Instr. and Meth. A 502 (2003) 266.

[13] J. Va'vra, M. Schneider, M. McCulloch (FCRID), unpublished.

[14] J. Va'vra et al. (CRID), Nucl. Instr. and Meth. A 433 (1999) 59.

[15] A. Di Mauro (DELPHI), Nucl. Instr. and Meth. A 433 (1999) 190.

[16] T. Ulalland, private communication.

[17] D.R. Broemmelsiek (HERA-B), Nucl. Instr. and Meth. A 433(1999)136.

[18] J.Va'vra, R. Kirby, M.McCulloch (SuperB R&D), 2011, unpublished.

[19] M. Hoek, private communication.

[20] M. Hoek (PANDA), Nucl. Instr. and Meth. A 639(2011)227.

[21] J. Cohen-Tanugi et al. (DIRC), Nucl. Instr. and Meth. A 515 (2003) 680.

[22] J. Va'vra, DIRC note #129, April 2000.

[23] J. Schwiening (Panda), private communication.

[24] M. Tabaka, Belle-II Aerogel RICH development, this conference

[25] A.F. Danilyuk et al., Nucl. Instr. and Meth. A 494(2002)491

[26] E. Kravchenko, Novosibirsk Aerogel RICH, talk at this conference.

[27] T. Iijima (Belle-II), VCI2004, Feb. 2004.

[28] EMF company's data, Ithaca, NY 14850.

[29] E. Albrecht et al. (COMPASS), Nucl. Instr. and Meth. A 502 (2003) 236.

[30] H. Anderhub et al. (FACT), Nucl. Instr. and Meth. A 639 (2011) 58

[31] J. Va'vra et al. (FDIRC), Nucl. Instr. and Meth. A 718 (2013) 541.

[32] Corning Co. information, 2009

[33] J. Va'vra, SLAC-PUB 13464, November 17, 2008

[34] R. Gernhauser et al., Nucl. Instr. and Meth. A 371 (1996) 300.

[35] S. Biaggi, private communication.

[36] A. Yarritu, S. Spanier, and J. Va'vra (DIRC), IEEE Trans. on Nucl. Sci.,
    Vol. 49, No. 4, August 2002.

[37] S.W.S. McKeever, Thermo-luminescence of solids, Cambridge Solid
    State Science Series, Cambridge Univ. Press, Cambridge, 1988, p. 187.